JMEPEG (2004) 13:665-669
DOI: 10.1361/10599490421268

1059-9495/$19.00

Transformation Superplasticity in Zircadyne 705

Hipolito J. Gonzalez and David C. Dunand

(Submitted July 26, 2004)

The zirconium alloy Zircadyne 705 (main alloying addition: 2.5 wt.% Nb) was thermally cycled from 900 °C (100% β-phase) to 710 °C (80% α-phase and 20% β-phase), resulting in strain increments after each cycle that are linearly proportional to stress up to 2 MPa. Tensile elongations in excess of 240% were achieved without fracture. The Newtonian flow behavior and high ductility indicate that transformation superplasticity is the dominant deformation mechanism. The superplastic strain increment decreases as the cycling amplitude and period decrease, in general agreement with existing transformation superplasticity models.

Keywords creep, internal stresses, phase transformation, superplasticity, zirconium, Zr-705

1. Introduction

Transformation superplasticity can be activated in polymorphic materials that are thermally cycled about their phase transformation while simultaneously being subjected to an external stress. Unlike microstructural superplasticity, which relies on sliding of small (<10 μm) grains at constant temperature, transformation superplasticity is driven by internal mismatch stresses generated by the volumetric difference between the allotropic phases coexisting during the phase transformation, and is active at all grain sizes. Greenwood and Johnson predicted that a net plastic strain increment $\Delta\varepsilon$ is produced in the direction of the applied stress σ after each phase transformation as a result of the accommodation of the internal mismatch stresses σ_0 (averaged over both transformation time and spatial orientation of the phase transformation) of the plastically deforming weaker phase (Ref 1):

$$\Delta\varepsilon \approx \frac{2}{3} \cdot \frac{\Delta V}{V} \cdot \frac{\sigma}{\sigma_0} \cdot \frac{5 \cdot n}{(4 \cdot n + 1)} \quad \text{(Eq 1)}$$

where $\Delta V/V$ is the volume mismatch between the two phases, and n is the stress exponent of the creep law describing the plastic accommodation in the weaker phase. This equation has been found to accurately describe transformation superplasticity at low applied stresses in the technologically relevant pure metals iron (Ref 1-3), cobalt (Ref 1, 4), titanium (Ref 1, 5), and zirconium (Ref 1, 6) and in the iron- and titanium-based alloys (Ref 2, 7-9). To date, transformation superplasticity in zirconium-base alloys has not been studied, with the exception of a single recent article on Zircaloy 4 (Zr-1.5wt.%Sn) (Ref 10).

The purpose of this article is to investigate transformation superplasticity for another technologically relevant zirconium alloy, Zircadyne 705, which contains 2.5 wt.% Nb as the main alloying element. Superplastic forming of this alloy may find applications for shaping of objects used in the chemical processing industry.

2. Experimental Procedures

Rods of Zircadyne 705 (Zr-705) were procured from Teledyne Wah-Chang (Albany, OR), which provided the following alloy chemical composition (wt.%): Nb: 2.5%, Fe + Cr < 0.2%, H < 0.005%, N < 0.025%, C < 0.05%, O < 0.18% (this nonnuclear grade alloy can also contain up to 4.5% Hf). Cylindrical tensile specimens were machined to a gage length of 30 mm and gage diameter of 3 mm. The specimen heads were threaded with a length of 5 mm and a diameter of 4 mm, allowing for a small head-to-gage volume ratio.

All mechanical tests were performed under pure flowing argon in a custom-built creep frame outfitted with radiant heaters, as described in more detail in Ref 6. The specimen temperature was measured with a K-type thermocouple coated with boron-nitride. The specimen elongation was measured by a linear voltage-displacement transducer (LVDT) at the cold end of the load train.

Prior to all thermal cycling experiments, the specimen was allowed to achieve a steady-state creep rate at T_u = 900 °C (in the β-Zr phase, Fig. 1) under a stress of 1 MPa. A first series of thermal cycling experiments was performed where the lower cycle temperatures were varied from T_l = 620 °C to T_l = 860 °C (within the α + β phase region, Fig. 1), while maintaining a constant stress σ = 1 MPa, a constant upper cycle temperature T_u = 900 °C, and a constant cycling frequency ν = 1.67 h^{-1} (36 min/cycle). The cycles consisted of the following segments: (a) cooling from T_u = 900 °C to T_l in 3 min (corresponding to a cooling rate of $\Delta T/3$ K/min, where $\Delta T = T_u - T_l$); (b) holding for 15 min at T_l; (c) heating to T_u = 900 °C in 3 min; and (d) holding for 15 min at T_u. At this low cycling frequency, the long isothermal hold times ensured that transformation was complete. The strain increment per cycle $\Delta\varepsilon_{tot}$ was obtained by dividing the specimen gage de-

This paper was presented at the International Symposium on Superplasticity and Superplastic Forming, sponsored by the Manufacturing Critical Sector at the ASM International AeroMat 2004 Conference and Exposition, June 8-9, 2004, in Seattle, WA. The symposium was organized by Daniel G. Sanders, The Boeing Company.

Hipolito J. Gonzalez and **David C. Dunand,** Department of Materials Science and Engineering, 2220 Campus Dr., Northwestern University, Evanston, IL 60208. Contact e-mail: Dunand@northwestern.edu.

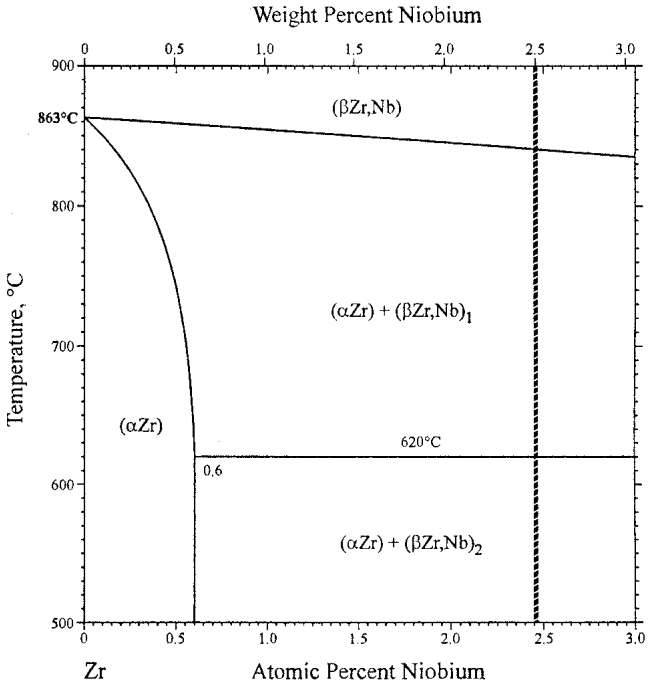

Fig. 1 Zr-Nb phase diagram (Ref 14) with Zr-2.5Nb composition (close to Zr-705)

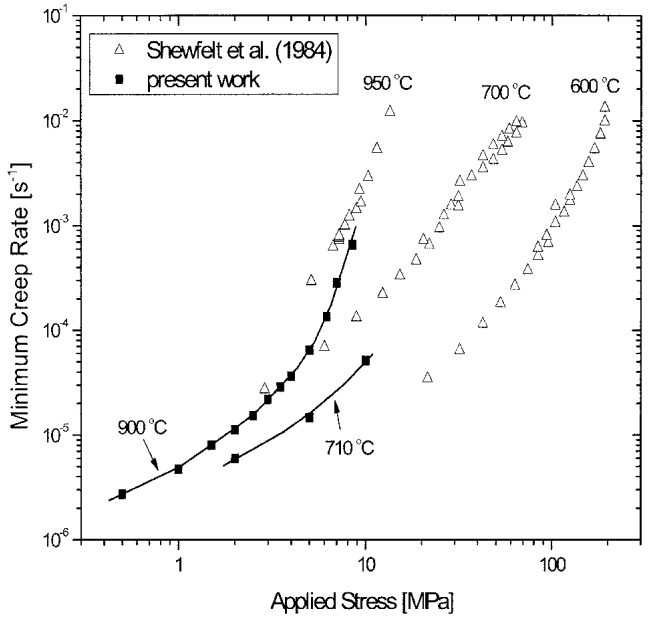

Fig. 2 Isothermal creep rate as a function of applied stress at 710 and 900 °C for Zr-705. Also shown are data from Shewfelt et al. (Ref 11) for Zr-2.5wt.%Nb at 600, 700, and 950 °C

formation increment (measured by the LVDT) after a full cycle with the gage length at the start of each cycle, calculated by assuming uniform plastic deformation of the gage length. A total of three to five cycles were performed for each temperature range ΔT, and an average strain increment was calculated after discarding the first cycle value, for which dynamical steady state was not achieved.

A second set of experiments consisted of varying the cycling frequency from $\nu = 1.67$ to 10 h^{-1} while maintaining a fixed upper and lower temperature ($T_u = 900$ °C, $T_l = 710$ °C) and a constant stresses of $\sigma = 1$ or 1.5 MPa. The cycling frequency was changed by varying the holding times at T_u and T_l from 0 to 15 min, while maintaining a constant ramp rate of 190/3 = 63 K/min.

A third set of experiments was performed in which the stress was varied between 0.5 and 3.5 MPa, under constant upper and lower temperatures ($T_u = 900$ °C, $T_l = 710$ °C) and frequency ($\nu = 3\ h^{-1}$), with holding times at T_u and T_l of 7 min. One specimen was deformed to fracture under a stress maintained between 1.5 and 2 MPa, under the same cycling conditions as above ($T_u = 900$ °C, $T_l = 710$ °C, and $\nu = 3\ h^{-1}$).

Control isothermal creep experiments were also conducted at 710 and 900 °C. The stress was maintained constant until a minimum creep rate was achieved and then increased to a higher level. Each specimen provided 3 to 5 creep data points.

3. Results

Figure 2 is a plot of the isothermal minimum creep rate versus applied uniaxial stress at 710 °C (α + β phases) and 900 °C (β phase). At 900 °C, the stress exponent increases continuously from ~1 to ~6 over the stress range 0.5 to 7 MPa. At 710 °C, the stress exponent is constant at ~1.3 over the measured stress range 2 to 10 MPa.

Figure 3 shows the average strain increment per cycle as a function of the applied stress with a fixed temperature amplitude ($T_u = 900$ °C, $T_l = 710$ °C) and fixed cycling frequency $\nu = 3\ h^{-1}$. A linear relationship is observed for stresses up to 2 MPa.

Figure 4 depicts the average strain increment per cycle as a function of the cycling amplitude ($T_u - T_l$) at a constant applied stress $\sigma = 1$ MPa, upper cycling temperature $T_u = 900$ °C, and cycling frequency of $\nu = 1.67\ h^{-1}$, low enough to ensure that the transformation was complete. This plot shows that the average strain per cycle increases near linearly with increasing temperature amplitude.

Figure 5 is a plot of the average strain increment per cycle as a function of the cycling frequency with a fixed temperature amplitude ($T_u = 900$ °C, $T_l = 710$ °C) and applied stress $\sigma = 1.5$ MPa. It is apparent from this plot that the transformation strain decreases rapidly with increasing cycle frequency.

Figure 6 shows two specimens deformed, respectively, under isothermal, creep conditions ($T = 900$ °C, $\sigma = 0.5$ to 8.2 MPa) and thermal cycling, superplastic conditions ($T = 710$ to 900 °C, $\sigma = 1.5$ to 2 MPa). The crept specimen fractured at an engineering strain of 114%, while the superplastic specimen achieved a tensile ductility of 243% without fracture.

4. Discussion

In Fig. 2, the isothermal creep behavior of Zr-705 measured at 710 and 900 °C is compared with previous data from Shewfelt et al. (Ref 11) for cold-worked Zr-2.5wt.%Nb at 600, 700, and 950 °C. As expected, creep rates at 900 °C are

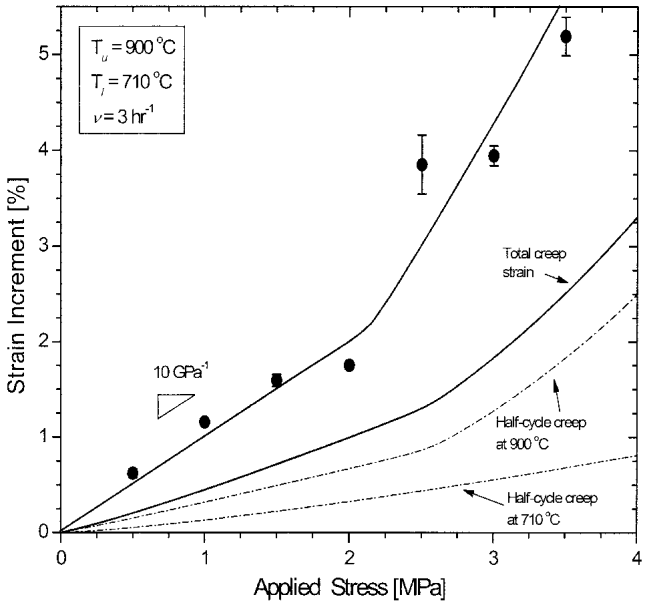

Fig. 3 Strain increment per cycle as a function of applied stress (T_l = 710 °C, T_u = 900 °C, ν = 3 h^{-1}). Also shown are calculated creep strains accumulated during 10 min (a half cycle) at T_l and T_u and their sum.

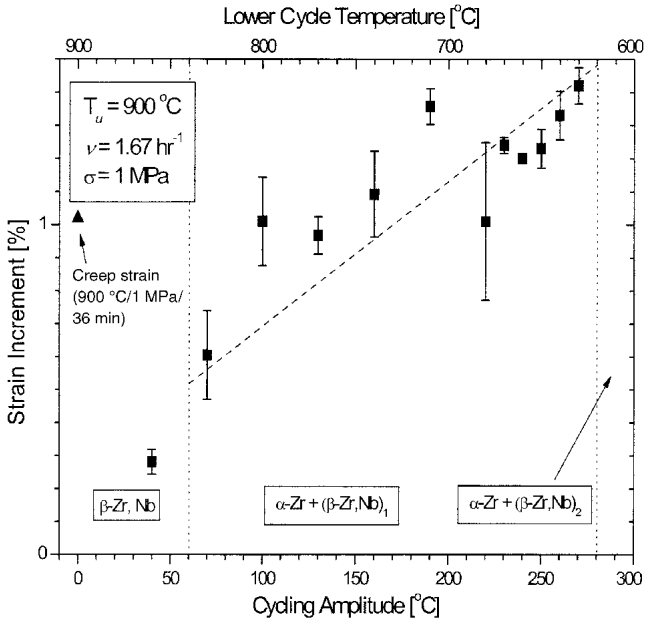

Fig. 4 Strain increment per cycle as a function of cycling amplitude (T_u – T_l) at constant upper temperature T_u = 900 °C (ν = 1.67 h^{-1}, σ = 1 MPa). Also shown is the calculated creep strain accumulated during 36 min (a full cycle) at T_u.

lower than those measured by Shewfelt et al. (Ref 11) at 950 °C. The smooth increase of stress exponent from ~1 to ~6 over the stress range 0.5 to 7 MPa can be attributed to the onset of diffusional creep at ~5 MPa. Similarly, the low stress exponent values at 700 and 710 °C are indicative of diffusional creep active well above 50 MPa (when considering the 700 °C

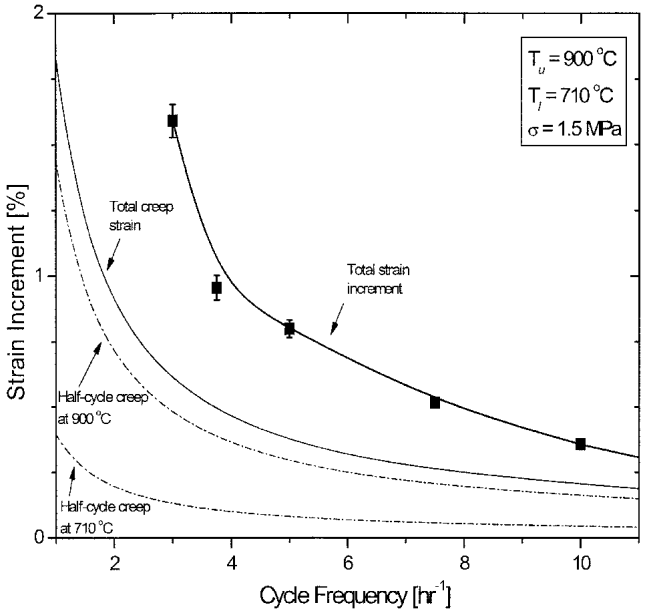

Fig. 5 Strain increment per cycle as a function of cycling frequency (T_l = 710 °C, T_u = 900 °C, σ = 1.5 MPa). Also shown are calculated creep strains accumulated during a half cycle at T_l and T_u and their sum.

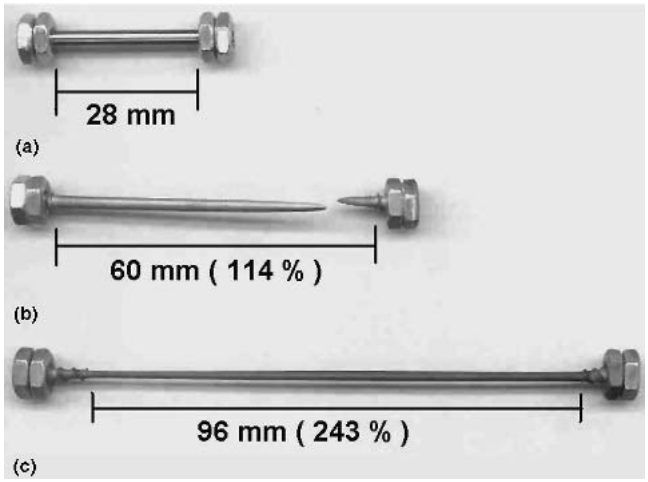

Fig. 6 Zr-705 specimens. (a) Before deformation. (b) After isothermal creep deformation at 900 °C (σ = 0.5 to 8.2 MPa), showing fracture. (c) After superplastic deformation by thermal cycling between 710 and 900 °C (σ = 1.5 to 2 MPa, ν = 3 h^{-1}), showing no fracture

data, Ref 11). The offset of strain rates between the authors' measurements at 710 °C and those of Shewfelt et al. (Ref 11) at 700 °C is most probably due to different grain sizes. Finally, the relatively small difference in the measured creep rates between 710 and 900 °C is indicative of the higher diffusivity (and thus lower creep resistance) of body-centered cubic β-Zr as compared with close-packed hexagonal α-Zr (Ref 12).

Figure 3 shows that the average strain increment per cycle increases linearly with applied stress up to 2 MPa, as expected from the linear relationship for transformation superplasticity

(Eq 1). The slope of the linear region is 10 GPa^{-1}. Also plotted in Fig. 3 is the strain that would have accumulated during one half cycle at the upper cycle temperature (T_u = 900 °C) and at the lower cycle temperature (T_l = 710 °C), using creep data in Fig. 2. The sum of these two contributions is an estimate of the creep strain that would have accumulated if there was no transformation superplasticity. It is apparent that, under thermal cycling conditions, the strain increments are higher than this calculated creep contribution, confirming that transformation superplasticity is active. Further evidence is provided by the following control experiment: when cycling the alloy between T_u = 900 °C and T_l = 860 °C (i.e., without phase transformation) with ν = 1.67 h^{-1} and σ = 1 MPa, a strain of 0.3% was accumulated. This is well below the strain increment of 1.15% achieved by allotropic thermal cycling (T_u = 900 °C and T_l = 710 °C) at the same stress (Fig. 3), despite the use of a higher frequency (ν = 3 h^{-1}) and a lower average temperature. Finally, the tensile ductility in excess of 243% (Fig. 6) is also a clear indication of transformation superplasticity.

If the estimated creep contribution is subtracted from the thermal cycling strain in Fig. 3, a linear slope of about 5 GPa^{-1} results at low stress. This value is close to the value of 4.4 ± 0.4 GPa^{-1} reported for unalloyed zirconium cycled between T_u = 910 °C and T_l = 810 °C (with a single allotropic transformation temperature at 863 °C), and ν = 6 to 10 h^{-1} (Ref 6). These results can also be compared with those of Gey et al. (Ref 10), who studied transformation mismatch plasticity of Zircaloy 4 (Zr-1.5wt.%Sn), which is characterized on heating by a transformation from an α-Zr(Sn) to a β-Zr(Sn) solid solution, starting at 850 and ending at 922 °C. The strain per half cycle (on heating) was found to increase linearly with applied stress up to 8 MPa, with a slope of 1.6 GPa^{-1}. Assuming the same contribution on the cooling half cycle, their slope for a full cycle is 3.2 GPa^{-1}. The discrepancy with 5 GPa^{-1} may be due to the difference in transformation temperatures (610-855 °C for Zr-705 and 850-922 °C for Zircaloy 4). Another difference with the authors' experiments is the very rapid cycling rate (heating rate of 10 K/s and holding time of 10 s), which may lead to incomplete transformation and/or an increase in average transformation internal stress, thus decreasing the strain increment (Eq 1).

Figure 4 shows that the strain increment increases linearly with the cycling amplitude. The cycling amplitude scales with the volume fraction of transformed α-Zr, which is itself proportional to the volume mismatch $\Delta V/V$. Then, Eq 1 predicts that the strain increment should scale with the transformation range. Using the zirconium-niubium phase diagram to estimate the transformed volume fraction in Zr-705 for the various lower cycling temperatures, the strain increment in Fig. 4 is replotted in Fig. 7 as a function of the volume fraction of α-Zr. As expected from Eq 1, a near-linear relationship results. A similar behavior was observed in Ti-6Al-4V cycled between a fixed lower temperature (T_l = 840 °C, with 25% volume fraction β-Ti) and an upper temperature T_u varied from 860 to 980 °C (where 95% β-Ti exists) (Ref 8). The near-linear behavior in Fig. 7 was further reported in super-α_2 titanium aluminide (Ti-25Al-10Nb-3Mo-1V, at.%) cycled between a fixed upper temperature T_u = 1150 °C, 100% β-phase) and a lower temperature T_l = 1100 to 910 °C (50% β-Ti exists at 910 °C)

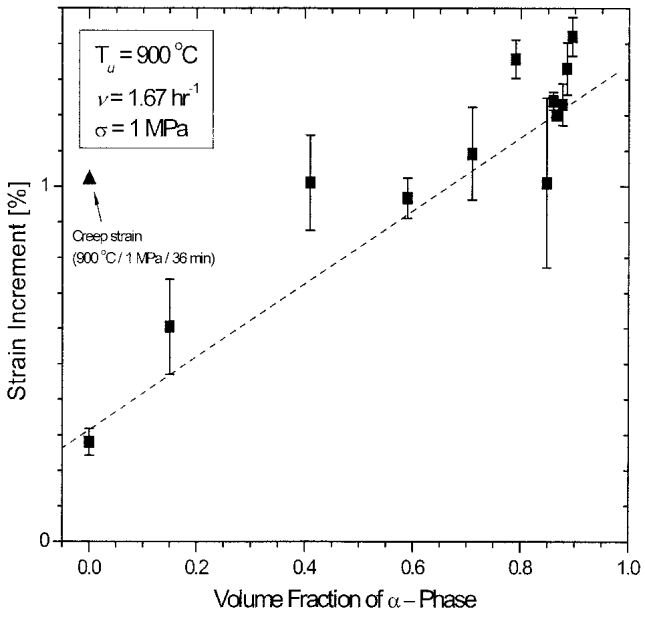

Fig. 7 Strain increment per cycle (experimental data from Fig. 4) as a function of estimated volume fraction of transformed of αZr

(Ref 13). In both studies (Ref 8, 13), models predicting a near-linear behavior between strain increment and volume fraction transformed were presented, but no attempt to quantitatively model the results was undertaken here, since the necessary input parameters for Zr-705 were not available, for example, temperature dependence of volume mismatch in the α-β-field and the kinetics of the α-β transformation.

Figure 5 shows that the strain increment per cycle increases strongly with decreasing frequency, that is, with increasing cycle period. A strain increase is expected from the creep contribution, which increases linearly with the period, and an estimate of the creep contribution is plotted in Fig. 5 using the same approach as Fig. 3 (creep strain during a half cycle at T_u and T_l, and sum of these). Subtracting this estimated creep contribution from the strain per cycle provides the transformation plasticity contribution, plotted in Fig. 8, which is less sensitive to cycling frequency. If the creep correction is accurate, it can be concluded from Fig. 8 that the transformation kinetics are relatively sluggish, so that a longer cycling period provides more transformation and thus a larger strain increment. By contrast, for super-α_2 titanium aluminide cycled between 950 and 1150 °C over a range of frequency ν = 4 to 15 h^{-1}, the strain increments were found to be independent of frequency after correcting for the creep contribution, indicating that the transformation kinetics were fast compared with the cycling period. A similar situation was reported for unalloyed zirconium (Ref 6), for which the strain increments were constant for ν = 6 to 15 h^{-1} but decreased for the very rapid frequency of ν = 30 h^{-1}, where transformation was incomplete due to restricted kinetics of heat transfer and/or phase transformation. As compared with unalloyed zirconium, the present Zr-705 alloy transforms over much lower temperatures (610-855 °C versus 862 °C), and the composition of the β-phase varies from 2.5 wt.% Nb at T_u = 900 °C to about 12 wt.% at

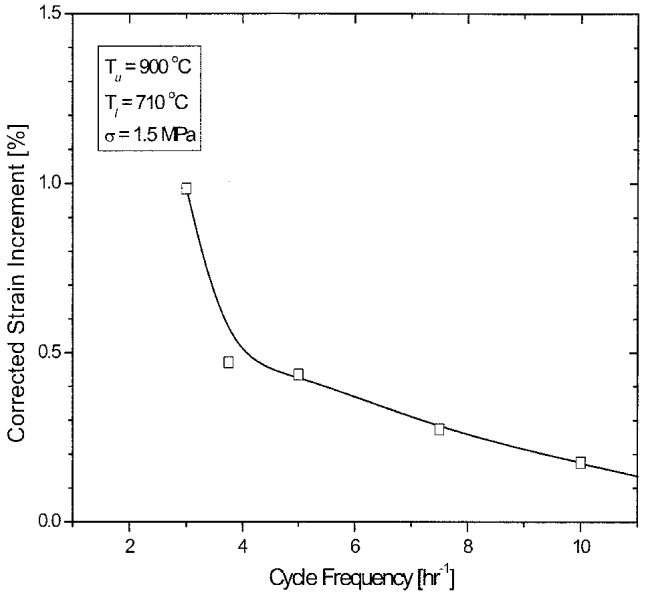

Fig. 8 Corrected strain increment per cycle (experimental data from Fig. 5 to which the creep strain was subtracted) as a function of cycling frequency (T_l = 710 °C, T_u = 900 °C, σ = 1.5 MPa)

T_l = 710 °C. Both effects are expected to decrease the transformation kinetics of Zr-705 as compared with unalloyed zirconium.

5. Conclusions

Transformation superplasticity was measured in Zircadyne 705 thermally cycled from 900 °C (in the β-Zr range) to various temperatures in the α-β-Zr range. A Newtonian flow behavior (strain increment per cycle is proportional to applied stress) is observed at low stresses, and strain increments can be accumulated up to a tensile deformation of 240% without fracture. The superplastic strain increment decreases as the cycling amplitude and period decrease, in general agreement with existing transformation superplasticity models.

Acknowledgment

This study was supported by National Science Foundation under Grant No. DMR-9987593. H.J.G. also acknowledges the support of the U.S. Nuclear Regulatory Commission through a NRC Graduate Fellowship.

References

1. G.W. Greenwood and R.H. Johnson, The Deformation of Metals Under Stress During Phase Transformations, *Proc. R. Soc. London,* Vol 283A, 1965, p 403-422
2. P. Zwigl and D.C. Dunand, Transformation Superplasticity of Iron and Fe/TiC Metal Matrix Composites, *Metall. Mater. Trans. A,* Vol 29, 1998, p 565-575
3. P. Zwigl and D.C. Dunand, A Numerical Model of Transformation Superplasticity for Iron, *Mater. Sci. Eng.,* Vol 262, 1999, p 166-172
4. J.P. Poirier, On Transformation Plasticity, *J. Geophys. Res.,* Vol 87, 1982, p 6791-6797
5. D.C. Dunand and C.M. Bedell, Transformation-Mismatch Superplasticity in Reinforced and Unreinforced Titanium, *Acta Mater.,* Vol 44, 1996, p 1063-1076
6. P. Zwigl and D.C. Dunand, Transformation Superplasticity of Zirconium, *Metall. Mater. Trans. A,* Vol 29, 1998, p 2571-2582
7. E. Gautier, A. Simon, and G. Beck, Transformation Plasticity During Perlitic Transformation of an Eutectoide Steel, *Acta Metall.,* Vol 35, 1987, p 1367-1375
8. C. Schuh and D.C. Dunand, Non-Isothermal Transformation-Mismatch Plasticity: Modeling and Experiments on Ti-6Al-4V, *Acta Mater.,* Vol 49, 2001, p 199-210
9. C. Schuh and D.C. Dunand, Tensile Fracture During Transformation Superplasticity of Ti-6Al-4V, *J. Mater. Res.,* Vol 16, 2001, p 865-875
10. N. Gey, E. Gautier, M. Humbert, A. Cerqueira, J.L. Bechade, and P. Archambault, Study of the Alpha/Beta Phase Transformation of Zy-4 in Presence of Applied Stresses At Heating: Analysis of the Inherited Microstructures and Textures, *J. Nucl. Mater.,* Vol 302, 2002, p 175-184
11. R.S.W. Shewfelt, L.W. Lyall, and D.P. Godin, A High-Temperature Creep Model for Zr-2.5 wt% Nb Pressure Tubes, *J. Nucl. Mater.,* Vol 125, 1984, p 228-235
12. P.M. Sargent and M.F. Ashby, Deformation Maps for Titanium and Zirconium, *Scr. Metall.,* Vol 16, 1982, p 1415-1422
13. C. Schuh and D.C. Dunand, Transformation Superplasticity of Super α2 Titanium Aluminide, *Acta Mater.,* Vol 46, 1998, p 5663-5675
14. H. Okamoto, Phase Diagrams of Dilute Binary Alloys, ASM International, 2002, p 301